

Original paper

Initial replacement stage of primary uranium (U^{IV}) minerals by supergene alteration: association of uranyl-oxide hydroxy–hydrates and “*calciolepersonnite*” from the Krátká Dolina Valley (Gemerská Poloma, Gemic Unit, Western Carpathians, Slovakia)

Štefan FERENC^{1*}, Adrián BIROŇ², Tomáš MIKUŠ², Ján SPIŠIAK¹, Šimon BUDZÁK³

¹ Department of Geography and Geology, Faculty of Natural Sciences, Matej Bel University, Tajovského 40, 974 01 Banská Bystrica, Slovak Republic; stefan.ferenc@umb.sk

² Earth Science Institute of the Slovak Academy of Sciences, Ďumbierska 1, 974 11 Banská Bystrica, Slovak Republic

³ Department of Chemistry, Faculty of Natural Sciences, Matej Bel University, Tajovského 40, 974 01 Banská Bystrica, Slovak Republic

* Corresponding author



Mineral association with uranyl-oxide hydroxy–hydrates and uranyl carbonate–silicates was found in J-1 quartz vein containing U–Au mineralization at Krátká Dolina Valley (Rožňava district, Slovakia). The vein penetrated Lower Palaeozoic graphitic phyllites and metalydites (Vlachovo Fm., Gemic Unit).

Among minerals identified at the site, becquerelite I is characterized by the highest Ca content and its composition is close to the ideal. On the other hand, becquerelite II is characterized by increased K at the expense of Ca. The average chemical composition of both types of becquerelite can be expressed by the empirical formulae: $(\text{Ca}_{0.85}\text{K}_{0.04}\text{Na}_{0.01}\text{Fe}_{0.02}\text{Zn}_{0.02}\text{Ba}_{0.01}\text{Pb}_{0.01})_{\Sigma 0.96}[(\text{UO}_2)_6\text{O}_4(\text{OH})_{5.84}] \cdot 8\text{H}_2\text{O}$ (becquerelite I) and $(\text{Ca}_{0.36}\text{K}_{0.27}\text{Na}_{0.01}\text{Fe}_{0.02}\text{Zn}_{0.02}\text{Pb}_{0.01}\text{Bi}_{0.01})_{\Sigma 0.78}[(\text{UO}_2)_6\text{O}_4(\text{OH})_{5.29}] \cdot 8\text{H}_2\text{O}$ (becquerelite II). Vandendriesscheite with unusual chemical composition imitates a transition phase between gauthierite and vandendriesscheite. Negative correlation of K vs. Pb indicates that in the studied mineral phase lead is partially replaced by potassium (and other cations). An average chemical composition of the studied vandendriesscheite can be expressed as: $(\text{K}_{0.49}\text{Na}_{0.02})_{\Sigma 0.51}(\text{Pb}_{1.20}\text{Fe}_{0.05}\text{Zn}_{0.04}\text{Ba}_{0.03}\text{Sr}_{0.02}\text{Al}_{0.02})_{\Sigma 1.36}[(\text{UO}_2)_{10}\text{O}_6(\text{SiO}_4)_{0.05}(\text{PO}_4)_{0.02}(\text{OH})_{10.86}] \cdot 11\text{H}_2\text{O}$. A leesite-like phase, with an average composition $(\text{K}_{0.72}\text{Sr}_{0.01}\text{Ba}_{0.02}\text{Fe}_{0.03}\text{Zn}_{0.01}\text{Pb}_{0.02}\text{Al}_{0.02})_{\Sigma 0.83}[(\text{H}_2\text{O})_2[(\text{UO}_2)_4\text{O}_2(\text{SiO}_4)_{0.01}(\text{OH})_{5.00}]_{\Sigma 11.01} \cdot 3\text{H}_2\text{O}$, was found only rarely. An unnamed mineral phase, with chemical composition close to lepersonnite-(Gd), designated as “*calciolepersonnite*”, is younger at the studied site than uranyl-oxide hydroxy–hydrates. Compared to the ideal lepersonnite-(Gd) formula, there is a lower REE content at the cationic position, an increased Ca and there are also monovalent cations (especially K) entering the structure. An average “*calciolepersonnite*” chemical composition is: $(\text{K}_{0.62}\text{Na}_{0.09})_{\Sigma 0.71}(\text{Ca}_{2.08}\text{Mg}_{0.04}\text{Sr}_{0.02}\text{Ba}_{0.02}\text{Fe}_{0.05}\text{Zn}_{0.05}\text{Pb}_{0.03})_{\Sigma 2.30}(\text{Y} + \text{REE})_{\Sigma 0.92}[(\text{UO}_2)_{23.76}\{(\text{SiO}_4)_{3.19}(\text{PO}_4)_{0.11}(\text{AsO}_4)_{0.02}(\text{SO}_4)_{0.02}\}_{\Sigma 3.34}(\text{CO}_3)(\text{OH})_{26.37}] \cdot 46.82\text{H}_2\text{O}$.

In the supergene zone of J-1 vein at Gemerská Poloma, three stages of development can be defined: (I) formation of uranyl-oxide hydroxy–hydrates that directly, partially or completely, replace U^{IV} minerals; (II) formation of uranyl carbonate–silicates (i.e., “*calciolepersonnite*”) that replace uranyl-oxide hydroxy–hydrates, apparently indicating shift to relative acid environment (but still remaining alkaline to neutral pH) and (III) formation of uranyl phosphates/arsenates of the autunite group (“uranium micas”) that precipitated relatively far from accumulations of primary (U^{IV}) minerals (in cracks and cavities of the gangue, or in the surrounding non-mineralized rocks). Their origin documents the change of alkaline–neutral to acidic environment, due the more advanced weathering of vein sulphides. Given the absence of Y + REE in older uranyl-oxide hydroxy–hydrates that directly replace brannerite, most of these elements required for “*calciolepersonnite*” formation were probably released from the host rocks and not from the primary, hydrothermal uranium minerals.

Keywords: uranyl-oxide hydroxy–hydrates, lepersonnite-(Gd), brannerite oxidation, uranyl minerals, Gemic Unit, Western Carpathians

Received: 1 March, 2018; accepted: 24 August, 2018; handling editor: J. Sejkora

1. Introduction

Uranium mineralization is common in almost all of the main tectonic units of the Western Carpathians, but the economic parameters reaches only in the Gemic, and less so in the Hronic and Tatic units. Uraninite is the dominant primary mineral at all occurrences of U ores.

Common uraninite guides are brannerite and coffinite, whereby the latter is known mainly from the U–Mo deposits in the Gemic Unit (Košice–Kurišková, Novoveská Huta). Brannerite is a dominant at the occurrence Petrova Hora Mts. near Krompachy (Gemic Unit), and common in Kálnica and Selec deposits in the Tatic Unit (Rojkovič 1997). It also occurs in the hydrothermal

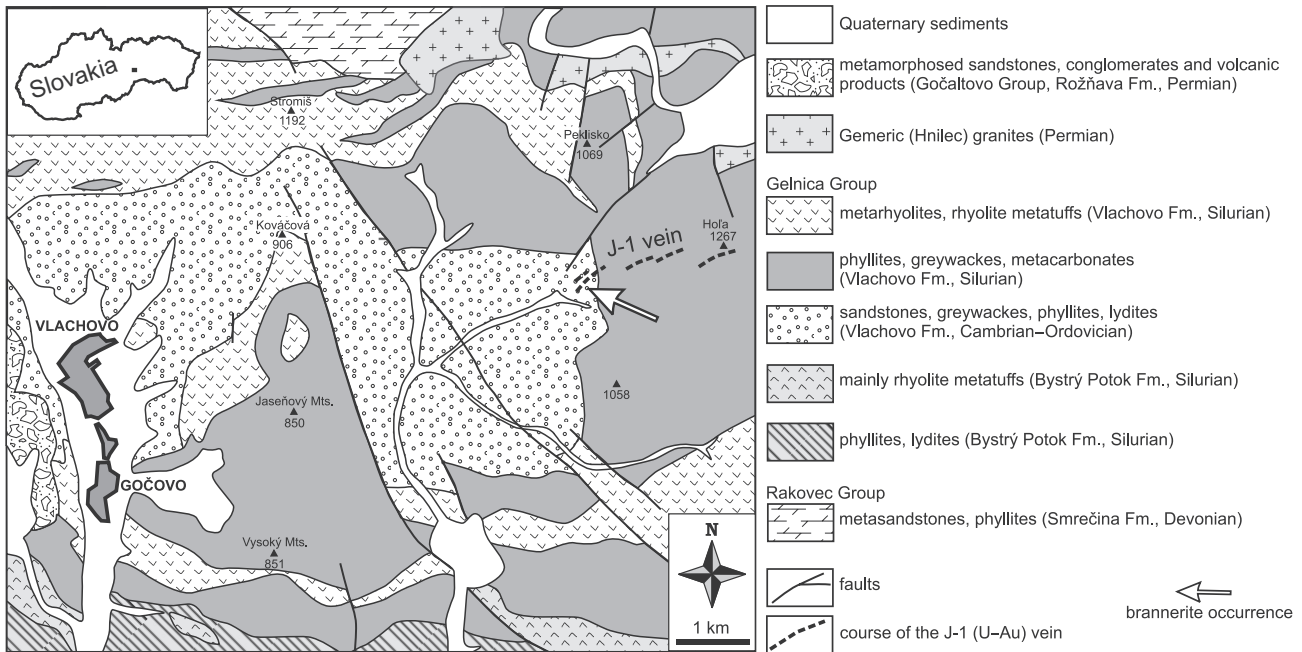


Fig. 1 Simplified geological map of the J-1 vein surroundings (according to Bajaník et al. 1984).

systems connected with the Cretaceous Rochovce granite intrusion (Poller et al. 2001; Kohút et al. 2013). The most interesting occurrences of brannerite represent Gemicic quartz (\pm apatite) veins that contain U–REE mineralization in the Krátka Dolina Valley (near Gemerská Poloma), Peklisko (at the Hnilec village), and at the end of the Gelnická Dolina Valley (Zimná Voda occurrence) near Prakovce (Novotný and Čížek 1979; Rojkovič and Novotný 1993; Rojkovič et al. 1997; Novotný et al. 1999; Donát et al. 2000).

Primary uranium (U^{IV}) minerals occurring on Slovak U mineralizations are mostly very fine-grained only. For this reason, it is difficult to observe the initial stage of their oxidation – *in-situ* replacing by mixed (U^{IV})–(U^{VI}) minerals or by uranyl-oxyde hydroxy–hydrates. Only the veins with U–REE mineralization in the Gemicic Unit (Krátka Dolina, Peklisko, Zimná voda) provided macroscopic samples of uraninite and brannerite (usually up to 1 cm, rarely up to 10 cm in size) that are often replaced by markedly yellow uranyl minerals, forming partial to full pseudomorphs. At the Gemerská Poloma–Krátka Dolina occurrence, a quartz gangue with massive accumulations of brannerite was found in the debris material. The present contribution deals with the mineralogical characteristics of supergene uranyl minerals that partially replace the massive, primary ore.

2. Geological setting

The Krátka Dolina U–Au vein mineralization occurrence is located in the Gelnica Group of the Gemicic Unit.

This Unit consists of a system of north-vergent nappes composed mainly of metamorphosed pre-Carboniferous complexes and Upper Palaeozoic to Lower Triassic syn- and post-orogenic formations (e.g. Maheľ and Vozár 1971; Németh et al. 2000; Radvanec and Grecula 2016). Most often it is divided into the Northern (Klátov, Rakovec, Črmel' and Ochtiná groups) and Southern (Gelnica and Štós groups) parts. The Gelnica Group is represented by a several thousand meters thick Palaeozoic volcanogenic (rhyolite–dacite) flysch (Snopko and Ivanička 1978; Ivanička et al. 1989), and its origin was associated with an active margin of Gondwana (Vozárová 1993; Putiš et al. 2008). Both sedimentary and volcanic rocks have undergone regional metamorphism under the chlorite zone of the greenschist-facies conditions (Faryad 1991a, b). The Gelnica Group (from the bottom to top) is divided into Vlachovo, Bystrý Potok and Drnava formations (*sensu* Bajaník et al. 1983, 1984; Ivanička et al. 1989) intruded by the Permian Gemicic granites. Although according to geological maps the Bystrý Potok Fm. is stratigraphically assigned to the Silurian, its magmatic rocks yielded Middle–Late Ordovician U–Th–Pb SHRIMP zircon ages of 465.8 ± 1.5 Ma (Putiš et al. 2008; Vozárová et al. 2010), 460–465 Ma respectively (Vozárová et al. 2017).

Vein J-1 with U–Au mineralization is located c. 15 km N of the district town Rožňava, on the south-facing slope of Krátka Dolina Valley. Massive brannerite was found in the eastern part of the vein, 8.6 km to the NNE from Gemerská Poloma village, 7 km to the ENE from Vlachovo village, 2 km to the WSW from the Hoľa Mts. (1267 m a. s. l.) at an altitude of about 700 m a. s. l. Geographical

coordinates of brannerite finding are N 48°47'14.9" and E 20°30'21.5".

The surroundings of occurrence are built mainly by the Vlachovo Fm. (Cambrian–Silurian; Fig. 1). It is formed by metarhyolites and rhyolite metatuffs; metasediments are represented mainly by phyllites (sericite, quartz–sericite, chlorite–sericite and sericite–graphite); metamorphosed greywackes, sandstones, conglomerates, carbonates, and lydites are also present. According to the recent concept of the Gemic Unit (Grecula et al. 2009, 2011) were rocks of the Vlachovo Fm. divided into Betliar and Smolník formations (Ordovician–Devonian).

The J-1 vein consists of discontinuous structures (total length of 2.25 km) cutting the graphitic phyllites and metalydites of the Vlachovo Fm. (Donát et al. 2000). The individual segments have a length of 150–400 m, strike WSW–ENE to SW–NE and dip 38–60° to the SE. The vein has a lenticular character and very variable thickness (0.01–1 m). Dominant vein mineral is quartz, containing brannerite, uraninite, gold, pyrite, galena, chalcopyrite, bornite, pyrrhotite, arsenopyrite, marcasite, sphalerite, glaucodote, gersdorffite, bismuthinite, millerite, bravoite, rutile, apatite, chlorite and sericite. The supergene zone is characterized by the occurrence of goethite, fourmarierite, autunite and torbernite/metatorbernite (Varček 1977; Rojkovič and Novotný 1993; Ferenc et al. 2003). Uranium content in the gangue ranges from 0.08 to 6.57 wt. % (predominantly 0.1–0.88 wt. %), the maximum determined Au concentration was 17.2 ppm (Donát et al. 2000).

There are two fundamentally different views on the genesis of the quartz-(± apatite) veins with U–REE (±Au) mineralization in the Gemic Unit. Rojkovič (1997) and Rojkovič et al. (1995, 1999) considered mineralization as Hercynian, whereby the Permian Gemic granites presumably provided fluids and thermal energy. The hydrothermal effect of granites could have caused mobilization of P, REE and U from the surrounding Lower Palaeozoic graphitic phyllites, metalydites and metaphosphates, and subsequent concentration of these elements in the hydrothermal veins. Recent electron-microprobe U–Pb uraninite dating from Čučma by Števko et al. (2014) gave a Palaeoalpine age (207±2 Ma; Late Triassic). On this basis, Permian granites are still considered as a possible source of mineralization elements. However, mobilization of P, F, U, REE and Y from granites and their deposition in the hydrothermal veins had to occur during the Late Triassic tectonothermal rejuvenation of the Gemic Unit (Radvanec et al. 2009).

3. Methods

Yellow secondary uranium minerals were separated from the surface of brannerite sample to prepare pol-

ished sections and mounts for powder X-ray diffraction analysis (XRD) and Infrared spectroscopic analysis (IR) respectively.

X-ray diffraction analysis was performed on a Bruker D8 Advance equipment (Earth Science Institute of Slovak Academy of Sciences – SAS, Banská Bystrica, Slovakia) using CuK α (1.5418 Å) radiation generated at a voltage of 40 kV and a current of 30 mA. The powder mount was placed in an ethanol suspension onto a Si single crystal. Subsequently, diffraction data were obtained under the following conditions: apertures 0.3° – 6 mm – 0.3° – 0.2 mm, primary and secondary Soller aperture 2.5°, step 0.02° 2Θ/1.25 s, measuring range 2.0–65.0° 2Θ, EDS detector Sol-XE. Diffraction patterns were evaluated using the Difrac.Eva software (Bruker AXS 2010) and PDF2/2010 database. Individual reflections were indexed according to structural data available in Downs and Hall-Wallace (2003). Unit-cell parameters were calculated from the X-ray diffraction pattern by least-squares method, using the UnitCell software (Holland and Redfern 1997).

Becquerelite was also studied by IR spectroscopy in a spectral range from 4000 to 400 cm $^{-1}$, using a Nicolet iS50 equipment (Matej Bel University, Banská Bystrica, Slovakia), using conventional technique of Attenuated Total Reflection (ATR) with a synthetic diamond as a measuring crystal. During each measurement, 32 scans with step 0.482 cm $^{-1}$ were taken. The two empirical equations: $R_{U-O} = 106.5[v_1(UO_2)^{2+}]^{-2/3} + 0.575$ Å and $R_{U-O} = 91.41[v_3(UO_2)^{2+}]^{-2/3} + 0.804$ Å (Bartlett and Cooney 1989) were applied for the calculation of the U–O bond lengths in uranyl ion based on observed wavenumbers.

Electron probe micro-analysis (EPMA) of mineral phases was performed by the JEOL JXA-8530F equipment (Institute of the Earth Sciences SAS, Banská Bystrica, Slovakia). Following conditions were used: accelerating voltage 15 kV, probe current 15 nA and a beam diameter of 10 µm. The ZAF matrix correction was employed. The used X-ray lines, crystals, detection limits (in ppm) and natural/synthetic standards were: Ca (K α , PETL, 37–70) – diopside, K (K α , PETL, 45–50) – orthoclase, U (M β , PETL, 103–116) – UO $_2$, Th (M α , PETL, 75–79) – thorianite, Pb (M β , PETL, 126–173) – crocoite, S (K α , PETL, 46–53) – baryte, P (K α , PETL, 68–89) – apatite, Y (L α , PETL, 131–166) – YPO $_4$, F (K α , LDE1, 159–334) – fluorite, Na (K α , TAP, 68–126) – albite, Sr (L α , TAP, 120–269) – celestite, Si (K α , TAP, 82–95) – orthoclase, Al (K α , TAP, 52–60) – albite, As (L α , TAP, 133–257) – GaAs, Mg (K α , TAP, 48–101) – diopside, Lu (L α , LIFH, 204–210) – LuPO $_4$, Ho (L β , LIFH, 355–365) – HoPO $_4$, Yb (L α , LIFH, 186–189) – YbPO $_4$, Tm (L α , LIFH, 175–183) – TmPO $_4$, Er (L α , LIFH, 173–176) – ErPO $_4$, Gd (L β , LIFH, 283–293) – GdPO $_4$, Dy (L α , LIFH, 148–153) – DyPO $_4$, Tb (L α , LIFH, 130–138) – TbPO $_4$, Sm (L β , LIFH,

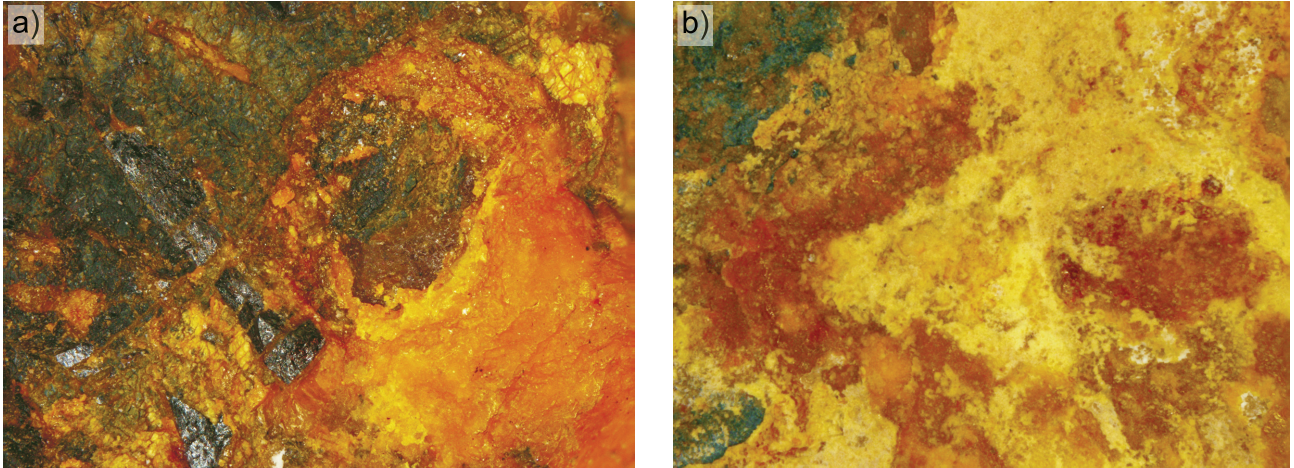


Fig. 2a – Brannerite (black) is replaced by the yellow–orange becquerelite. Horizontal width 4 mm. **b** – Light yellow coatings of uranyl-oxide hydroxy-hydrates (dominance of vandendriesscheite and “*calciolepersonnrite*”) grown on the orange becquerelite crust. Black mineral is brannerite. Horizontal width 3 mm.

251–269) – SmPO₄, Eu (L_a, LIFH, 130–135) – EuPO₄, Pr (L_β, LIFH, 230–242) – PrPO₄, Nd (L_a, LIFH, 123–127) – NdPO₄, Ce (L_a, LIFH, 121–130) – CePO₄, La (L_a, LIFH, 130–139) – LaPO₄, Co (K_a, LIFH, 94–109) – Co, Zn (K_a, LIF, 308–372) – gahnite, Cu (K_a, LIF, 214–253) – cuprite, Fe (K_a, LIF, 225–297) – olivine, Ti (K_a, LIF, 211–247) – rutile, Ba (L_a, LIF, 546–864) – baryte, Bi (M_a, PETJ, 310–664) – Bi₂Se₃.

X-ray element distribution maps of uranyl-oxide hydroxy-hydrates were obtained (the same device) with an accelerating voltage of 15 kV and probe current of 15 nA.

4. Nature of uranyl minerals

Uranyl minerals form conspicuously yellow coatings on the surface of the massive brannerite (+quartz) gangue, and fine crystalline crusts, with thickness up to 1 mm.

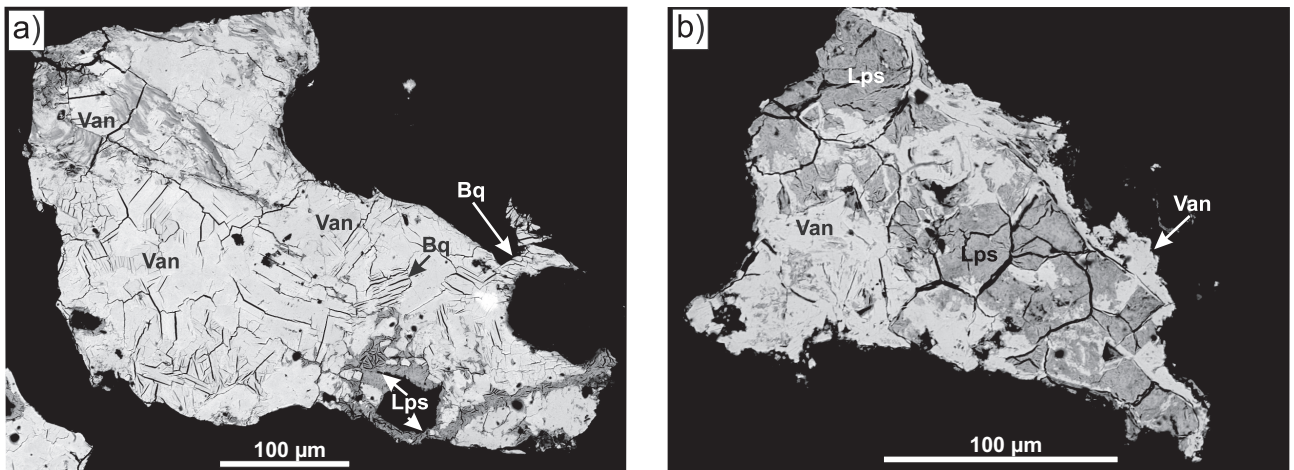


Fig. 3 Back-scattered electron images (BSE) of uranyl minerals from the Krátká Dolina Valley (Gemerská Poloma). **a** – Vandendriesscheite (Van) – becquerelite (Bq) aggregate is cut by the “*calciolepersonnrite*” veinlets (Lps). **b** – Intergrowth of “*calciolepersonnrite*” (Lps) and vandenriesscheite (Van).

They also fill hairline fissures in brannerite. Using binocular magnifier it can be observed that the crust consists of two layers.

The lower one that covers directly brannerite surface is microcrystalline to compact, with yellow–orange colour and greasy lustre (Fig. 2a). It is formed by becquerelite far predominant over vandendriesscheite and leesite-like phase.

The upper layer is microcrystalline, with pale yellow colour and matte lustre (Fig. 2b). It is composed of dominant vandendriesscheite and insignificant amount of becquerelite. Uranyl-oxide hydroxy-hydrates in both layers are accompanied by lepersonnite-like mineral (an unnamed uranyl carbonate-silicate), although it is more widespread in the upper layer.

On a microscopic scale, becquerelite and vandendriesscheite form irregular aggregates that are difficult to distinguish in the BSE mode. Both minerals have a relatively

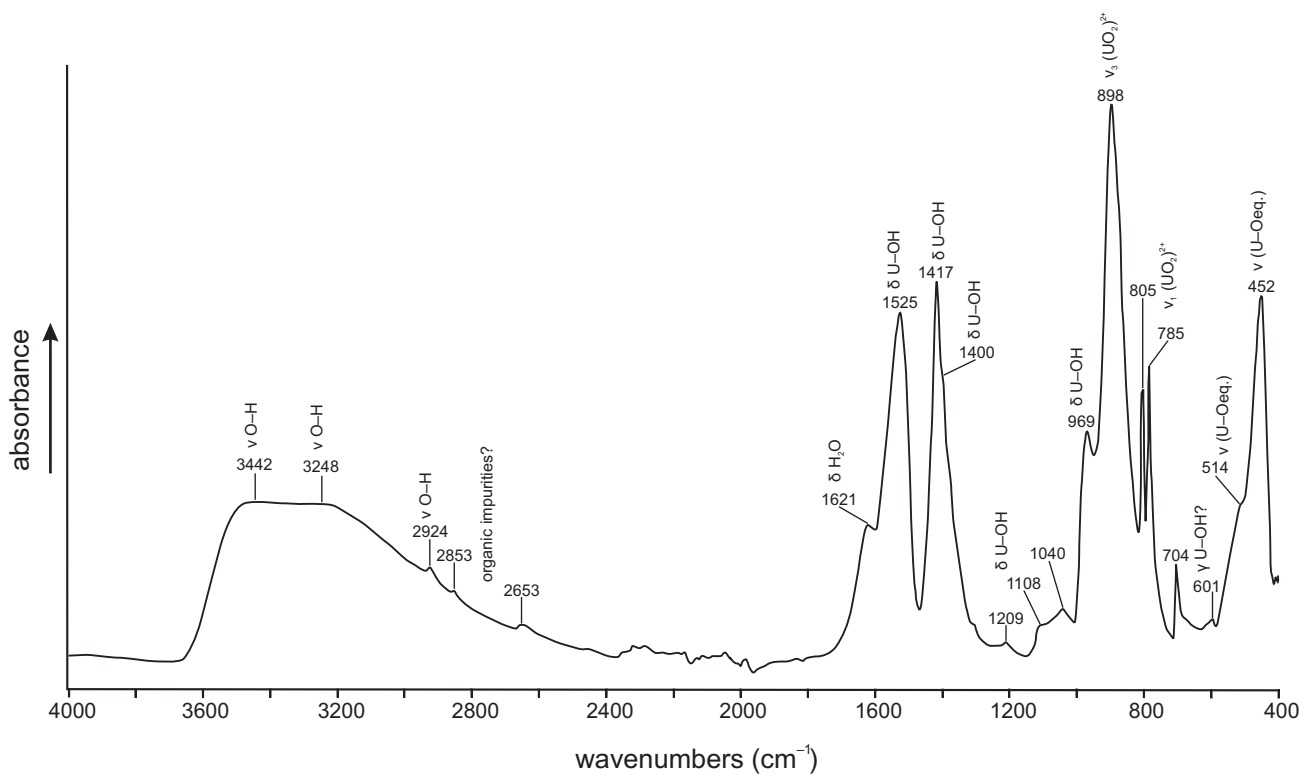


Fig. 4 Infrared spectrum of becquerelite from Gemerská Poloma.

Tab. 1 X-ray powder diffraction pattern of becquerelite from Gemerská Poloma

$I_{\text{obs.}}$	$d_{\text{obs.}}$	$d_{\text{calc.}}$	h	k	l
100.0	7.4683	7.4600	0	0	2
1.0	6.5728	6.5689	1	0	2
0.1	5.5972	5.5968	2	1	1
0.9	4.6817	4.6811	1	0	3
18.6	3.7324	3.7300	0	0	4
1.6	3.6014	3.6018	1	0	4
0.6	3.4582	3.4650	4	0	0
0.3	3.3782	3.3752	4	0	1
1.7	3.2019	3.1898	2	3	2
0.5	3.1379	3.1426	4	0	2
0.2	3.0974	3.0842	1	3	3
0.1	2.9550	2.9589	4	2	1
0.3	2.9173	2.9172	1	0	5
0.4	2.5701	2.5806	4	2	3
0.2	2.5377	2.5386	4	0	4
1.2	2.4873	2.4867	0	0	6
0.4	2.4480	2.4476	1	0	6
0.1	2.3841	2.3769	1	3	5
0.2	2.1082	2.1016	1	3	6
0.4	2.0378	2.0372	2	0	7
0.1	1.9356	1.9354	3	0	7
0.5	1.8668	1.8656	6	3	3
0.5	1.8504	1.8510	5	0	6
0.2	1.6133	1.6123	2	0	9

compact surface; in cases, they can be recognized by cleavage or fissure systems (Fig. 3a–b). Becquerelite is characterized by either parallel cracks or fissures arranged with an approximate angle of 120°. The cracks in vandendriesscheite adopt a zig-zag arrangement and, unlike becquerelite, do not prefer a specific direction. Both minerals locally intergrow intimately.

Becquerelite was identified by the XRD analysis, IR spectroscopy, and also by the EPMA. The XRD pattern of becquerelite from the Krátká Dolina Valley (Tab. 1) is in line with previously published data (Frondel and Cuttitta 1953; Protas 1957; Christ and Clark 1960; Piret-Meunier and Piret 1982; Pagoaga et al. 1987; Burns and Li 2002). The unit-cell parameters of the studied becquerelite and their mutual ratios (Tab. 2) correspond to the published data for this mineral ($a:b:c = 1.118:1:1.205$ – average calculated from a , b , c values in Tab. 2).

In the IR vibration spectrum of studied becquerelite (Fig. 4) several bands were detected. Split band with peaks at 805 and 785 cm⁻¹ can be connected with the $\nu_1(\text{UO}_2)^{2+}$ symmetric stretching vibration, the calculated U–O bond lengths in uranyl ion are 1.81 Å/805 cm⁻¹ and 1.83 Å/785 cm⁻¹, respectively. A band with a high intensity at 898 cm⁻¹ is related to the $\nu_3(\text{UO}_2)^{2+}$ antisymmetric stretching vibrations; the corresponding U–O bond length calculated from the observed stretching frequency is 1.79 Å. The obtained values of U–O bond lengths in the studied becquerelite are in agreement with

Tab. 2 Refined unit-cell parameters of becquerelite from Gemerská Poloma (orthorhombic space group $Pn2_1/a$)

	a [Å]	b [Å]	c [Å]	V [Å 3]	$a:b:c$
this work	13.837(1)	12.401(4)	14.926(1)	2561(1)	1.116:1:1.204
Billiet and de Jong (1935)	13.9	12.55	14.9	2600	1.108:1:1.187
Frondel and Cuttitta (1953)	13.92(1)	12.45(1)	15.09(1)	2615	1.118:1:1.212
Protas (1957)	13.86(3)	12.42(3)	14.96(3)	2575	1.116:1:1.205
Christ and Clark (1960)	13.86	12.38	14.96	2567	1.120:1:1.208
Piret-Meunier and Piret (1982)	13.86	12.3	14.92	2543.5	1.127:1:1.213
Pagoaga et al. (1987)	13.8378(9)	12.3781(12)	14.9238(9)	2556.2(1)	1.118:1:1.206
Burns and Li (2002)	13.8527(5)	12.3929(4)	14.9297(5)	2563.2(1)	1.118:1:1.205

published structure data (Pagoaga et al. 1987; Burns and Li 2002), or the results of the Raman spectroscopy study (Frost et al. 2007). Band at 452 cm $^{-1}$ with a shoulder at 514 cm $^{-1}$ may be assigned to the ν ($U-O_{\text{equatorial}}$) bending vibrations. Intense bands at 1525 and 1417 cm $^{-1}$, with a shoulder at 1400 cm $^{-1}$ were (sensu Frost et al. 2007) assigned to overtones or combination bands, but they may also be attributed to the δ U-OH bending vibrations. Weak bands at 1209, 1108, 1040, and 969 cm $^{-1}$ may also be connected with δ U-OH bending vibrations. Bands at the 704 and 601 cm $^{-1}$ probably represent the γ U-OH out-of-plane bending vibration or the water molecules librations. The δ H $_2$ O bending vibration is manifested by the band at 1621 cm $^{-1}$, bands at 3442, 3248 and 2924 cm $^{-1}$ may be assigned to the ν O-H stretching vibrations. Wavenumbers of the ν O-H vibrations were used for calculation of O-H···O hydrogen bond lengths (after Libowitzky 1999). The calculated hydrogen bond lengths $d(O\cdots O)$ 2.83 Å/3442 cm $^{-1}$; 2.72 Å/3248 cm $^{-1}$ and 2.63 Å/2924 cm $^{-1}$ correspond to rather strong hydrogen bonds. Weak bands at 2853 and 2653 cm $^{-1}$ may be

assigned to organic impurities in a sample. Overall, the spectrum is in a good agreement with published IR spectra of becquerelite (Čejka et al. 1998; Frost et al. 2007).

Based on their chemical composition, two types of becquerelite (I and II) can be distinguished in the samples studied. *Becquerelite I* (Tab. 3, analyses 1 to 6) is characterized by high CaO (average of 2.44 wt. %; 0.85 apfu Ca), and its composition is close to the ideal becquerelite formula (Fig. 5a–b); the total content of other divalent cations reaches 0.42 wt. % M^{2+} O (corresponding to 0.06 apfu M^{2+}). Only insignificant amount of K $_2$ O (average 0.18 wt. %; 0.04 apfu K) is present at the cationic (A) position. The average chemical composition of becquerelite I can be expressed by the empirical formula: $(Ca_{0.85}K_{0.04}Na_{0.01}Fe_{0.02}Zn_{0.02}Ba_{0.01}Pb_{0.01})_{\Sigma 0.96}[(UO_2)_6O_4(OH)_{5.84}] \cdot 8H_2O$.

Becquerelite II is characterized by increased K $_2$ O (average of 1.29 wt. %; 0.27 apfu K; Tab. 3, analyses 7–9) at the expense of CaO (c. 1.01 wt. %; 0.36 apfu Ca). Compared with becquerelite I, the M^{2+} content (excluding Ca) is slightly increased (average 0.40 wt. % M^{2+} O; 0.14 apfu M^{2+}). An elevated content of Bi (0.51 wt. % Bi $_2$ O $_3$; 0.02 apfu Bi) was found sporadically. Becquerelite II contains a higher proportion of compeignacite molecule in the structure (Fig. 5a–b); the average chemical formula can be expressed as: $(Ca_{0.36}K_{0.27}Na_{0.01}Fe_{0.02}Zn_{0.02}Pb_{0.01}Bi_{0.01})_{\Sigma 0.78}[(UO_2)_6O_4(OH)_{5.29}] \cdot 8H_2O$. The Si, P and As contents in

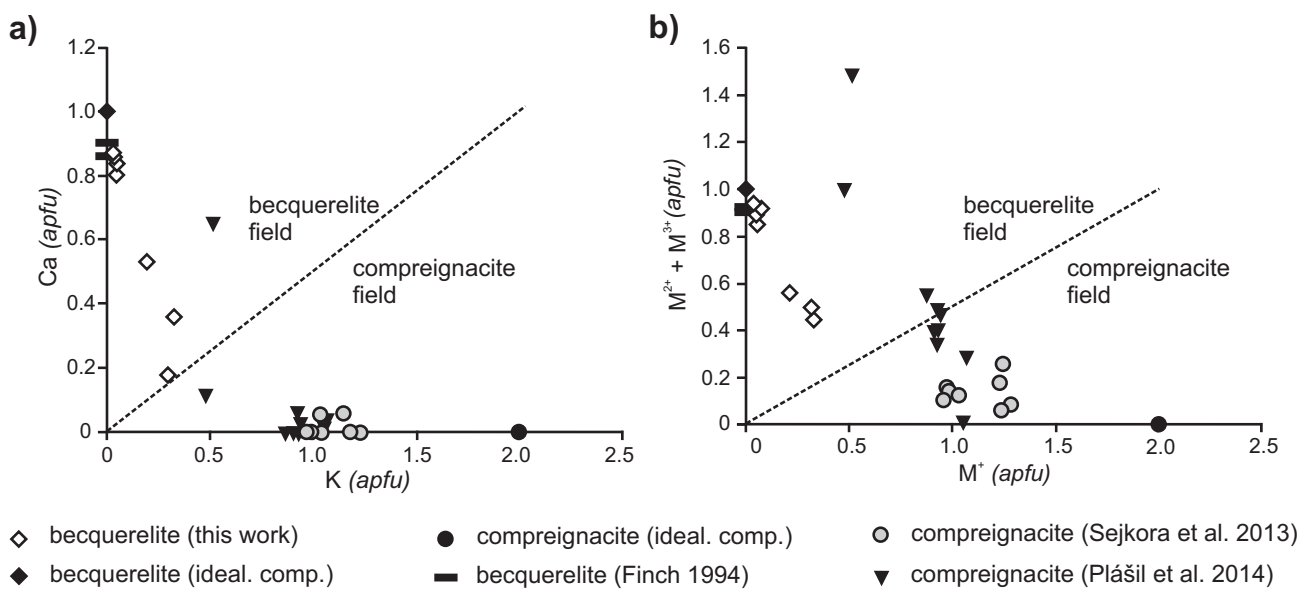


Fig. 5 Becquerelite compositions (apfu) from Gemerská Poloma compared to previously published data for becquerelite and compeignacite. **a** – K vs. Ca diagram. **b** – M^+ vs. $M^{2+} + M^{3+}$ diagram.

both types of becquerelite are negligible (below the respective detection limits).

Vandendriesscheite-like mineral was determined only by the microprobe analysis (Tab. 4). Vandendriesscheite can be expressed by the ideal formula $\text{Pb}_{1.5}(\text{UO}_2)_{10}\text{O}_6(\text{OH})_{11} \cdot 11\text{H}_2\text{O}$ (Vaes 1947; Burns 1997). In the samples studied, the dominant element in the cationic (A) position is Pb in variable concentrations (6.02–8.49 wt. % PbO ; 0.93–1.32 apfu Pb). Lead shows a significant negative correlation ($r = -0.78$) with the second most abundant element – potassium (Fig. 6a) (1.13–1.57 wt. % K_2O ; 0.43–0.58 apfu K). Contents of BaO , FeO , Al_2O_3 , and SiO_2 do not reach higher concentrations (<0.7 wt. % for each oxide; Tab. 4). These do not have a significant effect on the overall chemical composition of vandendriesscheite (Fig. 6b). The average chemical composition of the studied vandendriesscheite can be expressed as follows: $(\text{K}_{0.49}\text{Na}_{0.02})_{\Sigma 0.51}(\text{Pb}_{1.20}\text{Fe}_{0.05}\text{Zn}_{0.04}\text{Ba}_{0.03}\text{Sr}_{0.02}\text{Al}_{0.02})_{\Sigma 1.36}[(\text{UO}_2)_{10}\text{O}_6(\text{SiO}_4)_{0.05}(\text{PO}_4)_{0.02}(\text{OH})_{10.86}] \cdot 11\text{H}_2\text{O}$.

Tab. 3 Chemical composition of becquerelite from Gemerská Poloma (empirical formulae calculated on the basis of 6 U apfu)

	1	2	3	4	5	6	Mean	7	8	9	Mean
Na_2O	0.02	0.00	0.00	0.02	0.10	0.03	0.03	0.05	0.05	0.01	0.04
K_2O	0.17	0.15	0.22	0.20	0.19	0.14	0.18	0.95	1.39	1.52	1.29
CaO	2.45	2.57	2.43	2.18	2.46	2.57	2.44	1.54	0.50	1.00	1.01
SrO	0.00	0.02	0.00	0.00	0.00	0.00	0.00	0.00	0.02	0.00	0.01
BaO	0.21	0.00	0.00	0.14	0.21	0.00	0.09	0.00	0.00	0.00	0.00
FeO	0.08	0.15	0.14	0.00	0.05	0.10	0.09	0.00	0.23	0.07	0.10
ZnO	0.00	0.11	0.09	0.05	0.00	0.17	0.07	0.09	0.04	0.09	0.08
PbO	0.00	0.00	0.00	0.23	0.14	0.00	0.06	0.06	2.68	0.23	0.99
Bi_2O_3	0.00	0.00	0.00	0.09	0.00	0.00	0.02	0.00	0.00	0.51	0.17
SiO_2	0.00	0.00	0.00	0.00	0.07	0.00	0.01	0.00	0.00	0.00	0.00
P_2O_5	0.00	0.01	0.05	0.03	0.02	0.03	0.02	0.00	0.00	0.00	0.00
As_2O_5	0.00	0.00	0.03	0.01	0.00	0.00	0.01	0.06	0.02	0.00	0.03
UO_3	87.89	90.23	89.21	83.61	86.96	90.43	88.05	88.83	85.40	85.53	86.59
H_2O^*	8.14	8.13	8.14	8.13	8.11	8.13	8.13	8.19	7.00	8.17	7.79
$\Sigma \text{wt. \%}$	98.96	101.37	100.33	94.68	98.29	101.60	99.19	99.77	97.33	97.14	98.08
Na	0.005	0.000	0.000	0.007	0.031	0.009	0.009	0.015	0.017	0.003	0.012
K	0.036	0.030	0.045	0.043	0.039	0.027	0.037	0.195	0.297	0.324	0.272
Ca	0.851	0.872	0.835	0.799	0.864	0.871	0.849	0.531	0.178	0.359	0.356
Sr	0.000	0.004	0.000	0.000	0.000	0.000	0.001	0.000	0.005	0.000	0.002
Ba	0.027	0.000	0.000	0.019	0.026	0.000	0.012	0.000	0.000	0.000	0.000
Fe	0.023	0.039	0.038	0.000	0.013	0.027	0.023	0.000	0.065	0.020	0.028
Zn	0.000	0.027	0.022	0.011	0.000	0.040	0.018	0.022	0.011	0.023	0.019
Pb	0.000	0.000	0.000	0.021	0.012	0.000	0.005	0.005	0.241	0.021	0.089
Bi	0.000	0.000	0.000	0.004	0.000	0.000	0.000	0.000	0.000	0.022	0.007
$\Sigma \text{A site}$	0.942	0.971	0.940	0.905	0.986	0.975	0.953	0.768	0.814	0.772	0.784
SiO_4^{4-}	0.000	0.000	0.000	0.000	0.024	0.000	0.004	0.000	0.000	0.000	0.000
PO_4^{3-}	0.001	0.002	0.007	0.004	0.003	0.004	0.003	0.000	0.000	0.000	0.000
AsO_4^{3-}	0.000	0.000	0.003	0.001	0.000	0.000	0.001	0.005	0.001	0.000	0.002
$\Sigma \text{T site}$	0.001	0.002	0.010	0.005	0.027	0.004	0.008	0.005	0.001	0.000	0.002
UO_2^{2+}	6.000	6.000	6.000	6.000	6.000	6.000	6.000	6.000	6.000	6.000	6.000
OH^{**}	5.841	5.908	5.805	5.751	5.809	5.901	5.836	5.310	5.309	5.239	5.286
H_2O	8.000	8.000	8.000	8.000	8.000	8.000	8.000	8.000	8.000	8.000	8.000

H_2O^* – calculation based on the theoretical content of 8 H_2O in ideal becquerelite formula

OH^{**} – calculation based on the charge-balance

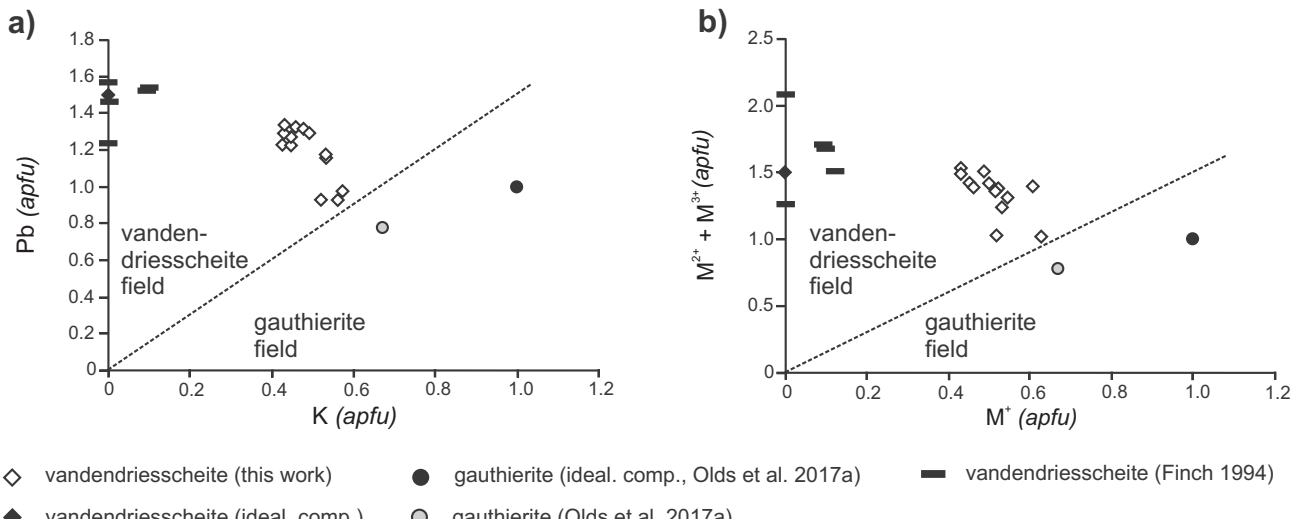


Fig. 6 Vandendriesscheite compositions (apfu) from the Gemerská Poloma compared with published data for vandendriesscheite and gauthierite. **a** – K vs. Pb diagram. **b** – M^+ vs. $M^{2+} + M^{3+}$ diagram.

Tab. 4 Chemical composition of vandendriesscheite from Gemerská Poloma (empirical formulae calculated on the basis of 10 U *apfu*)

	1	2	3	4	5	6	7	8	9	10	11	12	13	14	Mean
Na ₂ O	0.02	0.00	0.02	0.00	0.00	0.14	0.00	0.12	0.00	0.02	0.02	0.06	0.00	0.08	0.03
K ₂ O	1.45	1.14	1.18	1.25	1.16	1.20	1.13	1.55	1.43	1.35	1.31	1.57	1.48	1.30	1.32
CaO	0.00	0.00	0.00	0.00	0.00	0.00	0.00	0.00	0.01	0.00	0.00	0.00	0.00	0.00	0.00
SrO	0.15	0.06	0.00	0.03	0.06	0.09	0.00	0.00	0.07	0.04	0.06	0.03	0.01	0.00	0.04
BaO	0.00	0.31	0.00	0.00	0.08	0.18	0.55	0.00	0.00	0.00	0.22	0.36	0.00	0.00	0.12
FeO	0.14	0.11	0.15	0.06	0.08	0.00	0.12	0.08	0.04	0.09	0.16	0.33	0.05	0.10	0.11
ZnO	0.00	0.21	0.10	0.06	0.10	0.04	0.07	0.12	0.11	0.14	0.13	0.09	0.11	0.01	0.09
PbO	7.58	7.73	7.76	8.51	8.46	8.11	8.06	6.03	6.02	8.45	8.48	6.32	7.64	8.49	7.69
Bi ₂ O ₃	0.00	0.00	0.00	0.00	0.00	0.05	0.00	0.00	0.00	0.00	0.00	0.00	0.00	0.00	0.00
Al ₂ O ₃	0.03	0.12	0.19	0.00	0.11	0.00	0.00	0.00	0.00	0.00	0.00	0.36	0.00	0.00	0.06
SiO ₂	0.00	0.26	0.18	0.00	0.20	0.00	0.00	0.00	0.00	0.00	0.00	0.63	0.00	0.04	0.09
P ₂ O ₅	0.00	0.10	0.00	0.02	0.00	0.02	0.02	0.00	0.06	0.03	0.02	0.53	0.29	0.12	0.09
As ₂ O ₅	0.00	0.02	0.00	0.00	0.00	0.00	0.02	0.09	0.00	0.00	0.00	0.13	0.00	0.14	0.03
UO ₃	82.63	80.79	80.71	82.22	81.33	82.00	79.65	83.44	83.19	83.60	83.27	82.95	84.51	82.59	82.35
H ₂ O*	6.27	6.21	6.24	6.22	6.20	6.23	6.20	6.38	6.39	6.23	6.20	6.24	6.28	6.22	6.25
Σ wt. %	98.28	97.04	96.53	98.38	97.78	98.05	95.83	97.80	97.32	99.95	99.88	99.62	100.37	99.09	98.28
Na	0.013	0.000	0.009	0.000	0.000	0.077	0.000	0.067	0.000	0.010	0.011	0.032	0.000	0.045	0.019
K	0.533	0.430	0.444	0.461	0.433	0.445	0.430	0.563	0.520	0.491	0.478	0.575	0.532	0.479	0.487
Ca	0.000	0.000	0.000	0.000	0.000	0.000	0.000	0.000	0.006	0.000	0.000	0.000	0.000	0.000	0.000
Sr	0.051	0.020	0.000	0.010	0.020	0.029	0.000	0.000	0.025	0.014	0.021	0.010	0.004	0.000	0.015
Ba	0.000	0.071	0.000	0.000	0.018	0.041	0.129	0.000	0.000	0.048	0.082	0.000	0.000	0.028	
Fe	0.067	0.052	0.073	0.029	0.037	0.000	0.059	0.036	0.020	0.045	0.076	0.159	0.023	0.049	0.052
Zn	0.000	0.090	0.045	0.026	0.044	0.017	0.033	0.048	0.045	0.059	0.055	0.039	0.044	0.006	0.039
Pb	1.176	1.226	1.231	1.327	1.333	1.267	1.297	0.926	0.928	1.295	1.306	0.977	1.158	1.317	1.197
Bi	0.000	0.000	0.000	0.000	0.000	0.004	0.000	0.000	0.000	0.000	0.000	0.000	0.000	0.000	0.000
Al	0.008	0.042	0.066	0.000	0.039	0.000	0.000	0.000	0.000	0.000	0.000	0.120	0.000	0.000	0.020
Σ A site	1.850	1.931	1.868	1.852	1.924	1.880	1.947	1.640	1.543	1.914	1.994	1.995	1.762	1.895	1.857
SiO ₄ ⁴⁻	0.000	0.151	0.107	0.000	0.116	0.000	0.000	0.000	0.000	0.000	0.000	0.361	0.000	0.024	0.054
PO ₄ ³⁻	0.000	0.024	0.001	0.006	0.000	0.004	0.006	0.000	0.015	0.007	0.005	0.130	0.068	0.029	0.021
AsO ₄ ³⁻	0.000	0.002	0.000	0.000	0.000	0.000	0.004	0.014	0.000	0.000	0.000	0.020	0.000	0.021	0.004
Σ T site	0.000	0.177	0.108	0.006	0.116	0.004	0.010	0.014	0.015	0.007	0.005	0.511	0.068	0.073	0.080
UO ₂ ²⁺	10.000	10.000	10.000	10.000	10.000	10.000	10.000	10.000	10.000	10.000	10.000	10.000	10.000	10.000	10.000
OH**	11.161	10.791	10.917	11.226	10.990	11.229	11.435	10.608	10.522	11.306	11.484	9.611	10.788	10.023	10.864
H ₂ O	11.000	11.000	11.000	11.000	11.000	11.000	11.000	11.000	11.000	11.000	11.000	11.000	11.000	11.000	11.000

H₂O* – calculation based on the theoretical content of 11 H₂O in ideal vandendriesscheite formula

OH** – calculation based on the charge-balance

The mineral phase chemically close to *leesite* (Olds et al. 2018) was found only rarely. A leesite-like phase forms irregular grains, not exceeding 50 µm in size, enclosed by becquerelite and vandendriesscheite (see BSE image in Fig. 7). At the cationic (A) position, potassium is prevailing (2.58 wt. % K₂O; 0.72 *apfu* K; Tab. 5); the contents of BaO, FeO, ZnO and PbO are elevated only a little (0.0X–1 wt. %, for each oxide). The empirical formula of leesite-like mineral can be expressed as: (K_{0.72} Sr_{0.01} Ba_{0.02} Fe_{0.03} Zn_{0.01} Pb_{0.02} Al_{0.02})_{20.83}(H₂O)₂[(UO₂)₄O₂(SiO₄)_{0.01}(OH)_{5.00}]_{11.01}·3H₂O. The near-absence of Ca and Pb in leesite-like phase (Fig. 7) documents that this is not a “mixed” analysis of becquerelite and vandendriesscheite fine-intergrowths.

Unnamed mineral phase chemically close to *lepersonnite-(Gd)* was detected by EMPA. It is younger than the other uranyl-oxides hydroxy-hydrates, in which

it forms veinlets or irregular nests and often replaces them along the fissures (Fig. 3a–b). Lepersonnite-like mineral aggregates, up to 250 µm across, consist of needle-like crystals (up to 15 µm) arranged in fan-shape formations (Fig. 8a–b). The chemical composition of lepersonnite-like phase is given in Tab. 6. The Y + REE content ranges from 2.67 to 4.33 wt. % Y₂O₃ and REE₂O₃ (0.69–1.11 *apfu* Y + REE). Yttrium is low (max. 0.08 wt. % Y₂O₃; 0.03 *apfu* Y). Among REE, the dominant are Sm (1.07–1.55 wt. % Sm₂O₃; 0.28–0.40 *apfu* Sm) and Nd (0.71–1.30 wt. % Nd₂O₃; 0.19–0.36 *apfu* Nd). The average content of Gd₂O₃ is only 0.46 wt. % (0.11 *apfu* Gd). The concentrations each of the remaining REE (La, Ce, Pr, Eu, Tb, Dy, Tm, Yb) do not exceed 0.36 wt. % (for each element oxide). In the mineral structure, LREE (average 3.05 wt. % LREE₂O₃; 0.80 *apfu* LREE) dominate over HREE (average 0.42 wt. % HREE₂O₃;

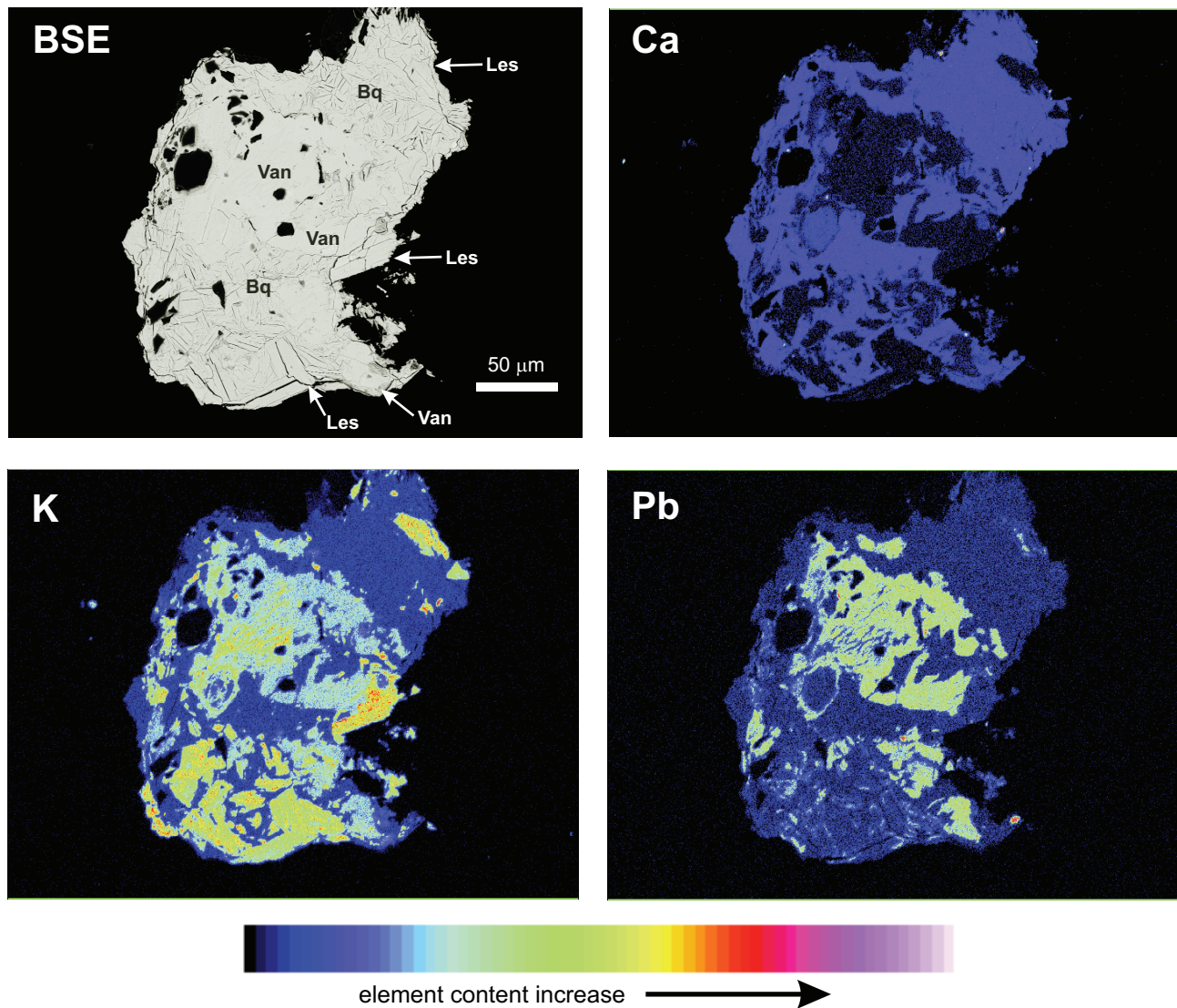


Fig. 7 Back-scattered electron (BSE) images and Ca, K and Pb X-ray element distribution maps of uranyl-oxide hydroxy–hydrates from Gemerská Poloma. Bq – becquerelite, Les – leesite-like phase, Van – vandendriesscheite.

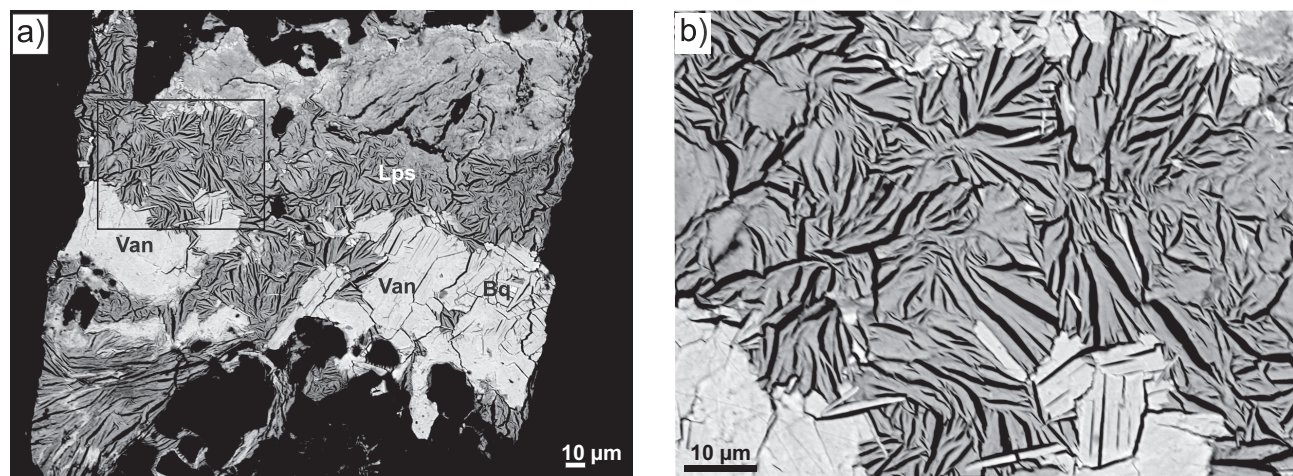


Fig. 8 Back-scattered electron (BSE) images of uranyl minerals from the Krátká Dolina Valley (Gemerská Poloma). **a** – “Calciolepersonnrite” (Lps) enclosing vandendriesscheite (Van) and becquerelite (Bq). **b** – Detailed view on the fan-shaped aggregates of “calciolepersonnrite” needle crystals.

Tab. 5 Chemical composition of leesite-like mineral phase from Gemerská Poloma (empirical formulae calculated on the basis of 4 U *apfu* and 20 O)

	1	2	3	Mean
Na ₂ O	0.02	0.00	0.00	0.01
K ₂ O	2.50	2.89	2.34	2.58
CaO	0.04	0.00	0.00	0.01
SrO	0.05	0.06	0.04	0.05
BaO	0.21	0.36	0.00	0.19
FeO	0.21	0.02	0.19	0.14
ZnO	0.05	0.12	0.11	0.09
PbO	1.01	0.00	0.13	0.38
Al ₂ O ₃	0.19	0.00	0.00	0.06
SiO ₂	0.18	0.00	0.00	0.06
UO ₃	86.98	90.40	82.63	86.67
H ₂ O*	10.00	10.74	9.80	10.18
Σ wt. %	101.43	104.59	95.23	100.42
Na	0.008	0.000	0.000	0.003
K	0.699	0.777	0.689	0.721
Ca	0.009	0.000	0.000	0.003
Sr	0.006	0.008	0.005	0.006
Ba	0.018	0.030	0.000	0.016
Fe	0.038	0.003	0.036	0.026
Zn	0.009	0.018	0.018	0.015
Pb	0.060	0.000	0.008	0.023
Al	0.050	0.000	0.000	0.017
Σ A site	0.895	0.836	0.755	0.829
SiO ₄ ⁴⁻	0.038	0.000	0.000	0.013
UO ₂ ²⁺	4.000	4.000	4.000	4.000
Total	4.934	4.836	4.755	4.842
O	20.000	20.000	20.000	20.000

H₂O* – calculation based on the 20 O in the ideal leesite formula

0.10 *apfu* HREE); of the latter, the most important is Tb (0.26 wt. % Tb₂O₃; 0.07 *apfu* Tb). Regarding the other elements present at the cationic (A) site, the most significant is Ca (0.99–1.64 wt. % CaO; 1.64–2.62 *apfu* Ca), which shows a strong positive correlation with Y + REE (*r* = +0.59). Potassium content varies in the range 0.48–0.89 wt. % K₂O (0.47–0.86 *apfu* K). Monovalent elements (K + Na) show a slight negative correlation with Y + REE (*r* = −0.45), K is weakly negatively correlated with Ca + Y + REE (*r* = −0.31). Thus, in this mineral phase, Ca and REE may be both partially substituted by K. The content of other elements (Tab. 6) is insignificant and reaches only the first tenths of wt. % of oxides. The presence of carbon (qualitative) was proven by the non-standardized EDS analysis. The average chemical composition of studied lepersonnite-like mineral can be expressed as: (K_{0.62}Na_{0.09})_{Σ0.71}(Ca_{2.08}Mg_{0.04}Sr_{0.02}Ba_{0.02}Fe_{0.05}Zn_{0.05}Pb_{0.03})_{Σ2.30}(Y + REE)_{Σ0.92}[(UO₂)_{23.76}{(SiO₄)_{3.19}(PO₄)_{0.11}(AsO₄)_{0.02}(SO₄)_{0.02}}_{Σ3.34}(CO₃)₈(OH)_{26.37}]·46.82H₂O. The studied unnamed mineral shows a deficiency in anionic

content (an average of 0.66 *apfu* Si + P + As + S; Tab. 6), compared to the ideal composition of lepersonnite-(Gd), Ca(REE)₂(UO₂)₂₄(SiO₄)₈(CO₃)₈(OH)₂₄·48H₂O (Deliens and Piret 1982).

5. Discussion and conclusions

5.1. Notes on the chemical composition of vandendriesscheite and lepersonnite-like phases

From the thirty known natural uranyl-oxide hydroxy-hydrates (28 mineral species stated in Plášil 2014, 2017 + shinkolobweite; Olds et al. 2017b and kroupaite; Plášil et al. 2017), ten contain Pb as a fundamental constituent (richetite, masuyite, spriggite, fourmarierite, meta-vandendriesscheite, sayrite, wölsendorfite, curite and shinkolobweite). Potassium, as an essential component, is present in four minerals only (agrinierite, compreignacite, rameauite and leesite).

In natural Pb-rich uranyl-oxide hydroxy-hydrates, potassium is usually present only as an admixture; e.g., ~0.25 wt. % K₂O were found in vandendriesscheite from Shinkolobwe, Congo (Finch 1994). More significant potassium contents have not yet been reported for vandendriesscheite. Until now, there are only two phases to contain both Pb and K as the essential constituents: gauthierite KPb[(UO₂)₇O₅(OH)₇]·8H₂O (Olds et al. 2017a) and kroupaite KPb_{0.5}[(UO₂)₈O₄(OH)₁₀]·10H₂O (Plášil et al. 2017). Both elements may also be present at significant amounts in calciouranoite.

Compared to the ideal vandendriesscheite (~10.2 wt. % PbO; 1.5 *apfu* Pb), the Pb content in the mineral phase from the Gemerská Poloma is lower (average of 7.69 wt. % PbO; 1.2 *apfu* Pb; Tab. 4) and an average K₂O content reaches 1.32 wt. % (0.49 *apfu* K). The studied vandendriesscheite with its unusual chemical composition imitates a transition phase between gauthierite and vandendriesscheite (Fig. 6a–b) approaching that of the natural gauthierite (see electron-microprobe analysis in Olds et al. 2017a). But there cannot exist a series of solid-solutions with variable K : Pb ratios between these minerals, due to their different crystal structure (see Burns 1997; Olds et al. 2017a). Negative correlation of K with Pb indicates that in the Gemerská Poloma vandendriesscheite, lead is partially replaced by potassium (and other cations). For the uranyl-oxide hydroxy-hydrates, this is unusual. For example, fourmarierite (general formula Pb_{1-x}[(UO₂)₄O_{3-2x}(OH)_{4+2x}]·4H₂O; Li and Burns 2000) in which potassium is introduced into the cationic position (0.70–1.56 wt. % K₂O; 0.20–0.45 *apfu* K) was found so far only in Jáchymov deposit, Czech Republic (Sejkora et al. 2013).

Tab. 6 Chemical composition of "calciolepersonnrite" from Gemerská Poloma (empirical formulae calculated on the basis of 31 apfu)

	1	2	3	4	5	6	7	8	9	10	11	12	13	Mean
Na ₂ O	0.08	0.06	0.16	0.00	0.02	0.06	0.09	0.01	0.01	0.06	0.13	0.04	0.05	0.06
K ₂ O	0.74	0.81	0.56	0.48	0.58	0.58	0.62	0.53	0.58	0.76	0.62	0.89	0.56	0.64
MgO	0.00	0.04	0.02	0.02	0.04	0.03	0.00	0.02	0.00	0.03	0.00	0.00	0.01	0.02
CaO	0.99	1.12	1.17	1.27	1.21	1.21	1.38	1.05	1.46	1.44	1.41	1.31	1.64	1.28
SrO	0.05	0.00	0.06	0.00	0.00	0.03	0.00	0.03	0.10	0.00	0.00	0.06	0.02	0.03
BaO	0.00	0.00	0.00	0.00	0.09	0.00	0.00	0.00	0.00	0.00	0.00	0.40	0.00	0.04
FeO	0.00	0.04	0.00	0.13	0.00	0.00	0.12	0.00	0.10	0.02	0.15	0.00	0.00	0.04
ZnO	0.05	0.12	0.00	0.18	0.00	0.08	0.07	0.00	0.00	0.00	0.00	0.00	0.05	0.04
PbO	0.11	0.00	0.00	0.00	0.00	0.00	0.00	0.05	0.00	0.20	0.04	0.43	0.08	0.07
Y ₂ O ₃	0.02	0.08	0.03	0.01	0.00	0.00	0.03	0.05	0.03	0.02	0.05	0.00	0.00	0.02
La ₂ O ₃	n.a.	0.05	0.03	0.00	0.01	0.10	0.00	0.02						
Ce ₂ O ₃	n.a.	0.21	0.19	0.14	0.20	0.14	0.16	0.08						
Pr ₂ O ₃	n.a.	0.18	0.18	0.02	0.07	0.05	0.00	0.04						
Nd ₂ O ₃	0.92	0.71	1.09	1.30	1.07	1.17	1.21	1.06	1.20	1.03	1.04	0.94	1.19	1.07
Sm ₂ O ₃	1.09	1.07	1.51	1.16	1.27	1.39	1.47	1.48	1.56	1.28	1.55	1.11	1.37	1.33
Eu ₂ O ₃	n.a.	0.11	0.13	0.12	0.16	0.10	0.15	0.06						
Gd ₂ O ₃	0.52	0.39	0.20	0.52	0.51	0.47	0.50	0.40	0.52	0.43	0.45	0.47	0.56	0.46
Tb ₂ O ₃	0.20	0.29	0.36	0.26	0.32	0.22	0.25	0.23	0.15	0.17	0.29	0.34	0.30	0.26
Dy ₂ O ₃	0.18	0.12	0.02	0.00	0.00	0.00	0.10	0.03	0.11	0.09	0.04	0.10	0.06	0.06
Tm ₂ O ₃	n.a.	0.12	0.07	0.11	0.06	0.15	0.09	0.05						
Yb ₂ O ₃	n.a.	0.03	0.16	0.04	0.11	0.11	0.22	0.05						
SiO ₂	1.95	1.94	2.26	2.10	2.20	2.21	2.24	2.12	2.30	2.03	2.10	1.84	2.11	2.11
P ₂ O ₅	0.00	1.39	0.02	0.05	0.04	0.03	0.02	0.01	0.00	0.04	0.03	0.52	0.00	0.17
As ₂ O ₅	0.16	0.14	0.05	0.00	0.01	0.02	0.00	0.00	0.06	0.02	0.00	0.06	0.02	0.04
SO ₃	0.03	0.07	0.04	0.01	0.00	0.02	0.01	0.01	0.01	0.01	0.00	0.02	0.01	0.02
UO ₃	75.24	75.02	72.84	74.40	73.81	76.71	74.72	73.73	75.33	74.53	75.71	74.15	74.66	74.68
CO ₂ *	4.80	4.76	4.77	4.77	4.78	4.78	4.75	4.73	4.85	4.82	4.82	4.82	4.85	4.79
H ₂ O*	14.74	14.60	14.63	14.64	14.66	14.68	14.58	14.52	14.88	14.81	14.81	14.88	14.71	
Σ wt. %	101.85	102.77	99.80	101.32	100.61	103.68	102.17	100.73	104.00	102.21	103.82	102.97	103.04	102.23
Na	0.123	0.085	0.246	0.000	0.030	0.091	0.134	0.018	0.007	0.089	0.180	0.051	0.072	0.087
K	0.728	0.773	0.553	0.471	0.570	0.551	0.595	0.529	0.542	0.728	0.584	0.855	0.530	0.616
Mg	0.005	0.078	0.046	0.048	0.099	0.056		0.044		0.077		0.007	0.024	0.037
Ca	1.644	1.787	1.948	2.082	2.005	1.932	2.220	1.754	2.314	2.328	2.239	2.113	2.619	2.076
Sr	0.048		0.055			0.024		0.025	0.083			0.052	0.017	0.023
Ba	0.000			0.051						0.000	0.000	0.237		0.022
Fe	0.049			0.168			0.154		0.120	0.024	0.184			0.054
Zn	0.054	0.131		0.207	0.000	0.090	0.082					0.060	0.048	
Pb	0.047						0.019		0.082	0.016	0.173	0.033	0.029	
Y	0.007	0.031	0.011	0.004			0.010	0.019	0.012	0.006	0.019		0.009	
La							0.015	0.009	0.001	0.002	0.027		0.004	
Ce							0.060	0.052	0.038	0.055	0.039	0.044	0.022	
Pr							0.050	0.049	0.007	0.020	0.014		0.011	
Nd	0.253	0.190	0.302	0.356	0.294	0.313	0.323	0.295	0.316	0.276	0.277	0.252	0.319	0.290
Sm	0.289	0.275	0.403	0.305	0.339	0.356	0.379	0.398	0.397	0.333	0.396	0.287	0.354	0.347
Eu							0.030	0.034	0.031	0.040	0.027	0.037	0.015	
Gd	0.133	0.096	0.052	0.131	0.130	0.117	0.125	0.103	0.127	0.107	0.110	0.116	0.138	0.114
Tb	0.051	0.072	0.090	0.065	0.082	0.055	0.062	0.058	0.037	0.043	0.071	0.085	0.073	0.065
Dy	0.045	0.029	0.004				0.025	0.007	0.025	0.021	0.009	0.025	0.014	0.016
Tm							0.029	0.016	0.025	0.013	0.036	0.020	0.011	
Yb							0.007	0.035	0.009	0.025	0.024	0.051	0.012	
Σ A site	3.425	3.596	3.710	3.836	3.600	3.585	4.109	3.459	4.176	4.226	4.239	4.420	4.406	3.910
Σ Y+REE	0.778	0.694	0.861	0.860	0.845	0.841	0.925	1.070	1.110	0.898	1.037	0.933	1.050	0.915
SiO ₄ ⁴⁻	3.012	2.898	3.504	3.217	3.403	3.297	3.351	3.306	3.400	3.069	3.113	2.772	3.146	3.191
PO ₄ ³⁻	0.874	0.015	0.034	0.029	0.016	0.010	0.009	0.001	0.022	0.018	0.331		0.105	
AsO ₄ ³⁻	0.065	0.053	0.021		0.004	0.008	0.023		0.007	0.024	0.007		0.016	
SO ₄ ²⁻	0.034	0.081	0.050	0.015		0.026	0.011	0.014	0.012	0.016	0.002	0.026	0.010	0.023
Σ T site	3.111	3.905	3.590	3.266	3.435	3.346	3.371	3.329	3.436	3.114	3.133	3.153	3.163	3.335
UO ₂ ²⁺	24.464	23.489	23.700	23.898	23.958	24.069	23.520	24.211	23.388	23.643	23.617	23.427	23.431	23.755
CO ₃ ²⁻ *	8.000	8.000	8.000	8.000	8.000	8.000	8.000	8.000	8.000	8.000	8.000	8.000	8.000	8.000
OH**	27.393	23.491	24.658	26.855	25.667	26.197	26.001	26.582	25.994	27.460	27.497	27.515	27.495	26.370
H ₂ O**	46.303	48.254	47.671	46.573	47.167	46.901	47.000	46.709	47.003	46.270	46.251	46.243	46.253	46.815

CO₃* and H₂O* – calculation based on the theoretical content of 8 CO₃ and 60 H₂O in ideal lepersonnite formulaOH** – calculation based on the charge-balance (at the expense of 60 H₂O, resulting in reduced H₂O content)

n.a. – not analysed

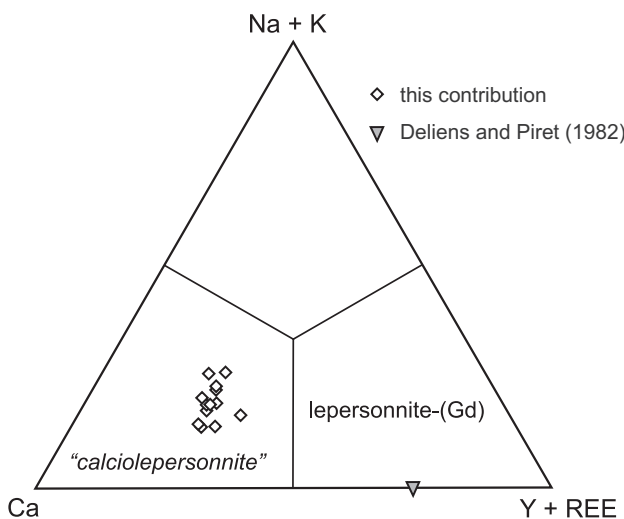


Fig. 9 Compositions of “*calciolepersonnrite*” from Gemerská Poloma compared with those of lepersonnite-(Gd) in ternary Ca–Na + K–Y + REE diagram (*apfu*).

Lepersonnrite $[\text{Ca}(\text{REE})_2(\text{UO}_2)_{24}(\text{SiO}_4)_4(\text{CO}_3)_8(\text{OH})_{24} \cdot 48\text{H}_2\text{O}]$, a mixed uranyl carbonate–silicate, was described from the Shinkolobwe deposit, Congo (Deliens and Piret 1982). According to the main element in the cationic (A) position, its name was modified to lepersonnrite-(Gd). Shinkolobwe until now remains the only locality with the occurrence of this rare mineral. The chemical composition of unnamed uranyl carbonate–silicate from Gemerská Poloma (Tab. 6) is notably similar to lepersonnrite-(Gd), but occupancy of the cationic position is distinct. Compared to the ideal formula of lepersonnrite-(Gd), the REE are lower and Ca higher; furthermore, there are monovalent cations (especially K) present. In the studied mineral, the ratios $M^+ : \text{Ca} : (\text{Y} + \text{REE})^{3+}$ and $M^+ : M^{2+} : (\text{Y} + \text{REE})^{3+}$ (*apfu*) are $1 : 2.95 : 1.30$ and $1 : 3.26 : 1.30$, respectively (Fig. 9). Thus, occupancy of the cationic (A) position suggests that the mineral phase from Gemerská Poloma could represent a calcium-dominant member of a broader mineral group, containing also lepersonnrite-(Gd). According to the principal element in the cationic position, it can be preliminarily named “*calciolepersonnrite*”, with an ideal formula $\text{KCa}_2(\text{REE})(\text{UO}_2)_{24}(\text{SiO}_4)_4(\text{CO}_3)_8(\text{OH})_{24} \cdot 48\text{H}_2\text{O}$. Significant positive correlations of Ca with $\text{Y} + \text{REE}$ ($r = 0.59$) and $\text{K} + \text{Na}$ (Fig. 9) indicate that it could also be a completely different mineral, not related to lepersonnrite-(Gd).

5.2. Origin of the uranyl oxide–hydroxy–hydrates and “*calciolepersonnrite*”

Up to now, a considerable research has been focused on the weathering processes of uranium mineralization under oxidation conditions. The evolution and classification of supergene changes of the primary U^{IV} minerals

has been summarized, for instance, in Ščerbina (1963), Belova (1975, 2000), Krivovichev and Plášil (2013) or Plášil (2014). Primary U^{IV} minerals are, at the very initial stage of their supergene weathering, replaced by ianthinite (presence of U^{4+} and U^{6+} in structure), and then by uranyl–oxide hydroxy–hydrates (schoepite, fourmarierite, becquerelite, vandendriesscheite etc.); uranyl silicates follow later.

The formation of all above secondary minerals takes place under alkaline to neutral conditions. They are suitable for the mobilization/transport of released uranium in the form of easily soluble mono-, di- and tricarbonate uranyl complexes (Langmuir 1978). Uranyl carbonates usually precipitate by evaporation of alkaline solutions at relatively high CO_2 fugacity (Finch and Murakami 1999), although they may also originate in a slightly acidic environment (*sensu* the scheme in Krivovichev and Plášil 2013).

Sulphide minerals form a rather broad association in quartz ± apatite veins with U, REE and Au mineralization in Lower Palaeozoic rocks of the Gemic Unit. Still, they are usually fine-grained and scattered, and only rarely they occur in larger accumulations (first centimetres in size) (Novotný and Čížek 1979; Rojkovič and Novotný 1993; Rojkovič et al. 1995, 1997, 1999; Novotný et al. 1999; Števko et al. 2014). As for uranium supergene minerals, the most abundant are uranyl arsenates/phosphates of the autunite group (uranium micas): autunite, torbernite, zeunerite, trögerite and probably kahlerite (Rojkovič 1997; Rojkovič et al. 1997, 1999). These minerals are typically formed under acidic conditions of weathering (Krivovichev and Plášil 2013 and references therein).

An analogous situation also occurs in the J-1 vein at Gemerská Poloma, from which comes the studied sample. Of the broad group of uranyl–oxide hydroxy–hydrates, only fourmarierite has been known from the studied site (confirmed by XRD analysis; Ferenc et al. 2003). Studied gangue is composed exclusively of brannerite and a small amount of quartz and uraninite, without sulphides. It represents exceptional accumulation of brannerite, which otherwise forms only small clusters of columnar crystals (up to 0.5 cm long) in the vein quartz. The association of uranyl–oxide hydrate–hydrates (becquerelite, leesite-like mineral, vandendriesscheite), which are accompanied by the younger mixed unnamed uranyl carbonate–silicate, “*calciolepersonnrite*”, has been identified in the yellow crusts on its surface. This mineral association indicates an alkaline to neutral environment of primary uranium (U^{IV}) weathering, due to the minimal content of sulphides in the gangue.

Based on the current results and field observations, three evolutionary stages of supergene mineral association can be described at the J-1 vein at Gemerská Poloma (following Finch and Ewing 1992 or Plášil et al. 2014):

(I) uranyl-oxide hydroxy-hydrates (fourmarierite, becquerelite, leesite-like phase, vandendriesscheite) partially or completely replace U^{IV} minerals; (II) an unnamed uranyl carbonate-silicate mineral ("calciolepersonnite") replaces uranyl-oxide hydroxy-hydrates, apparently indicating a shift towards relatively acid conditions and (III) uranyl phosphates/arsenates of the autunite group form [autunite, torbernite, zeunerite, trögerite (?), kahlerite (?)]. Relative to uranyl-oxide hydroxy-hydrates, these minerals precipitate relatively far from the accumulations of primary (U^{IV}) minerals (cracks and cavities in the gangue or in the surrounding non-mineralized rocks). Their origin documents the change of alkaline neutral to acidic environment, the latter due the more advanced weathering of vein sulphides (releasing the sulphuric acid).

The average Y + REE content in quartz veins containing U mineralization (Krátka Dolina–Peklisko occurrences) is 770 ppm (Rojkovič 1997). Since minerals such as monazite or xenotime are not abundant in the J-1vein, most of the Y + REE required for "calciolepersonnite" formation were probably released from the host rocks (Göb et al. 2013) and not from the primary, hydrothermal uranium or REE minerals. This is supported by the absence of Y + REE in older uranyl-oxide hydroxy-hydrates that directly replace brannerite.

Acknowledgements. This work was supported by the Slovak Research and Development Agency under the contract APVV-15-0050, as well as the Ministry of Education, Slovak Republic VEGA-1/0237/18 and VEGA-2/0023/17 projects. Authors thank to Travis A. Olds, Jakub Plášil and Martin Števko for precise reviews and improvement of the manuscript. Finally, we thank to Jiří Sejkora (Handling editor) and Vojtěch Janoušek (Editor-in-Chief) for their constructive suggestions.

References

- BAJANÍK Š, HANZEL V, MELLO J, PRISTAŠ J, REICHWALDER P, SNOPKO L, VOZÁR J, VOZÁROVÁ A (1983) Explanation to geological map of the Slovenské Rudohorie Mts. – eastern part, 1 : 50 000. State Geological Institute of D. Štúr, Bratislava, pp 1–223 (in Slovak)
- BAJANÍK Š, IVANIČKA J, MELLO J, REICHWALDER P, PRISTAŠ J, SNOPKO L, VOZÁR J, VOZÁROVÁ A (1984) Geological map of the Slovenské Rudohorie Mts. – eastern part, 1 : 50 000. State Geological Institute of D. Štúr, Bratislava (in Slovak)
- BARTLETT JR, COONEY RP (1989) On the determination of uranium–oxygen bond lengths in dioxouranium (VI) compounds by Raman spectroscopy. *J Mol Struct* 193: 295–300
- BELOVA LN (1975) Zones of Oxidation of Hydrothermal Uranium Deposits. Nedra, Moscow, pp 1–173 (in Russian)
- BELOVA LN (2000) Formation conditions of oxidation zones of uranium deposits and uranium mineral accumulations in the gipergenesis zone. *Geol Ore Dep* 42: 103–110
- BILLIET V, DE JONG WF (1935) Schoepite and becquerelite. *Naturw Tijdschr Ned-Indië* 17: 157–162 (in Dutch)
- BRUKER AXS (2010) Difrac.Eva – User Manual. Bruker AXS, Karlsruhe, pp 1–134
- BURNS PC (1997) A new uranyl oxide hydrate sheet in vandendriesscheite: implications for mineral paragenesis and the corrosion of spent nuclear fuel. *Amer Miner* 82: 1176–1186
- BURNS PC, LI Y (2002) The structures of becquerelite and Sr-exchanged becquerelite. *Amer Miner* 87: 550–557
- CHRIST CL, CLARK JR (1960) Crystal chemical studies of some uranyl oxide hydrates. *Amer Miner* 45: 1026–1061
- ČEJKA J, SEJKORA J, SKÁLA R, ČEJKA J, NOVOTNÁ M, EDEROVÁ J (1998) Contribution to the crystal chemistry of synthetic becquerelite, billietite and protasite. *Neu Jb Mineral, Abh* 174: 159–180
- DELIENS M, PIRET P (1982) Bijvoetite et lepersonnite, carbonates hydratés d'uranyle et de terres rares de Shinkolobwe, Zaire. *Canad Mineral* 20: 231–238
- DONÁT A, MIHÁL F, NOVOTNÝ L (2000) Geological-Exploration Works on the Au in Lower Paleozoic of Spišsko-Gemerské Rudohorie Mts. Unpublished Report, State Geological Institute of D. Štúr, Bratislava, pp 1–209 (in Slovak)
- DOWNS RT, HALL-WALLACE M (2003) The American Mineralogist Crystal Structure Database. *Amer Miner* 88: 247–250
- FARYAD SW (1991a) Metamorphism of the Early Paleozoic salic to intermediate volcanic rocks. *Miner Slov* 23: 325–332 (in Slovak)
- FARYAD SW (1991b) Metamorphism of the Early Paleozoic sedimentary rocks in Gemicum. *Miner Slov* 23: 315–324 (in Slovak)
- FERENC Š, ROJKOVIČ I, MAŤO L (2003) Uranyl minerals of Western Carpathians. In: ZIMÁK J (ed) Mineralogy of Bohemian Massif and Western Carpathians. Palacký University, Olomouc, pp 17–23 (in Slovak)
- FINCH JR (1994) Paragenesis and Crystal Chemistry of the Uranyl Oxide Hydrates. Unpublished PhD. Thesis, University of New Mexico, Albuquerque, pp 1–257
- FINCH JR, EWING RC (1992) The corrosion of uraninite under oxidizing conditions. *J Nucl Mater* 190: 133–156
- FINCH R, MURAKAMI T (1999) Systematics and paragenesis of uranium minerals. In: BURNS PC, FINCH R (eds) Uranium: Mineralogy, Geochemistry and the Environment. Mineralogical Society of America Reviews in Mineralogy 38: pp 91–179

- FRONDEL JW, CUTTITTA F (1953) Studies of uranium minerals (XII); The status of billietite and becquerelite. *Amer Miner* 38: 1019–1024
- FROST RL, ČEJKA J, WEIER ML (2007) Raman spectroscopic study of the uranyl oxyhydroxide hydrates: becquerelite, billietite, curite, schoepite and vandendriesscheite. *J Raman Spectrosc* 38: 460–466
- GÖB S, GÜHRING JE, BAU M, MARKL G (2013) Remobilization of U and REE and the formation of secondary minerals in oxidized U deposits. *Amer Miner* 98: 530–548
- GRECULA P, KOBULSKÝ J, GAZDAČKO Ľ, NÉMETH Z, HRAŠKO Ľ, NOVOTNÝ L, MAGLAY J (2009) Geological map of the Spišsko-Gemerské Rudohorie Mts., 1 : 50 000. State Geological Institute of D. Štúr, Bratislava (in Slovak)
- GRECULA P, KOBULSKÝ J, GAZDAČKO Ľ, NÉMETH Z, HRAŠKO Ľ, NOVOTNÝ L, MAGLAY J, PRAMUKA S, RADVANEC M, KUCHARIČ Ľ, BAJTOŠ P, ZÁHOROVÁ Ľ (2011) Explanations to geological map of the Spišsko-Gemerské Rudohorie Mts., 1 : 50 000. State Geological Institute of D. Štúr, Bratislava, pp 1–308 (in Slovak)
- HOLLAND TJB, REDFERN SAT (1997) Unit cell refinement from powder diffraction data: the use of regression diagnostics. *Mineral Mag* 61: 65–77
- IVANIČKA J, SNOPKO L, SNOPKOVÁ P, VOZÁROVÁ A (1989) Gelnica Group – Lower Unit of Spišsko-Gemerské Rudohorie Mts. (West Carpathians), Early Paleozoic. *Geol Zbor Geol Carpath* 40: 483–501
- KOHÚT M, STEIN H, UHER P, AIMMERMAN A (2013) Re–Os and U–Th–Pb dating of the Rochovce granite and its mineralization (Western Carpathians, Slovakia). *Geol Carpath* 64: 71–79
- KRIVOVICHEV SV, PLÁŠIL J (2013) Mineralogy and crystallography of uranium. In: BURNS PC, SIGMON GE (eds) *Uranium: From Cradle to Grave*, Mineralogical Association of Canada Short Courses 43: pp 15–119
- LANGMUIR D (1978) Uranium solution–mineral equilibria at low temperatures with applications to sedimentary ore deposits. *Geochim Cosmochim Acta* 42: 547–569
- LI Y, BURNS PC (2000) Investigation of crystal-chemistry variability in lead uranyl oxide hydrates II. Fourmarierite. *Canad Mineral* 38: 737–749
- LIBOWITZKY E (1999) Correlation of O–H stretching frequencies and O–H···O hydrogen bond lengths in minerals. *Monatsh Chem* 130: 1047–1059
- MAHEL M, VOZÁR J (1971) Contribution to knowledge of Permian and Triassic in the North-Gemeric syncline. *Geol Práce, Spr* 56: 47–66 (in Slovak)
- NÉMETH Z, PUTIŠ M, GRECULA P (2000) Tectonic evolution of Gemericum (the Western Carpathians) outlined by the results of petrotectonic research. *Miner Slov* 32: 169–172
- NOVOTNÝ L, ČÍŽEK P (1979) New occurrence of uranium–gold mineralization to the south of Prakovce in Spišsko-Gemerské Rudohorie Mts. *Miner Slov* 11: 188–190 (in Slovak)
- NOVOTNÝ L, HÁBER M, KRIŽÁNI I, ROJKOVIČ I, MIHÁL F (1999) Gold in the Early Paleozoic rocks in the central part of the Spišsko-Gemerské Rudohorie Mts. *Miner Slov* 31: 211–216 (in Slovak)
- OLDS TA, PLÁŠIL J, KAMPF AR, ŠKODA R, BURNS PC, ČEJKA J, BOURGOIN V, BOULLIARD JC (2017a) Gauthierite, $\text{KPb}[(\text{UO}_2)_7\text{O}_5(\text{OH})_7] \cdot 8\text{H}_2\text{O}$, a new uranyl-oxide hydroxy–hydrate mineral from Shinkolobwe with a novel uranyl-anion sheet-topology. *Eur J Mineral* 29: 129–141
- OLDS TA, LUSSIER AJ, OLIVER AG, PETŘÍČEK V, PLÁŠIL J, KAMPF AR, BURNS PC, DEMBOWSKI M, CARSON SM, STEELE IM (2017b) Shinkolobweite, IMA 2016-095. CNMNC Newsletter No. 36, April 2017, p 404; *Mineral Mag* 81: 403–409
- OLDS TA, PLÁŠIL J, KAMPF AR, SPANO T, HAYNES P, CARLSON SM, BURNS PC, SIMONETTI A, MILLS OP (2018) Leesite $\text{K}(\text{H}_2\text{O})_2[(\text{UO}_2)_4\text{O}_2(\text{OH})_5] \cdot 3\text{H}_2\text{O}$, a new K-bearing schoepite-family mineral from the Jomac mine, San Juan County, Utah, U.S.A. *Amer Miner* 103: 143–150
- PAGOAGA MK, APPLEMAN DE, STEWART JM (1987) Crystal structures and crystal chemistry of the uranyl oxide hydrates becquerelite, billietite, and protasite. *Amer Miner* 72: 1230–1238
- PIRET-MEUNIER J, PIRET P (1982) Nouvelle détermination de la structure cristalline de la becquerelite. *Bull Minéral* 105: 606–610
- PLÁŠIL J (2014) Oxidation–hydration weathering of uraninite: the current state-of-knowledge. *J Geosci* 59: 99–114
- PLÁŠIL J (2017) Uranyl-oxide hydroxy–hydrate minerals: their structural complexity and evolution trends. *Eur J Mineral* 30: 1–15
- PLÁŠIL J, SEJKORA J, ŠKODA R, ŠKÁCHA P (2014) The recent weathering of uraninite from Červená vein, Jáchymov (Czech Republic): a fingerprint of the primary mineralization onto the alteration association. *J Geosci* 59: 223–253
- PLÁŠIL J, KAMPF AR, OLDS TA, SEJKORA J, ŠKODA R, BURNS PC, ČEJKA J (2017) Kroupaite, IMA 2017-031. CNMNC Newsletter No. 38, August 2017, p 1036; *Mineral Mag* 81: 1033–1038
- POLLER U, UHER P, JANÁK M, PLAŠIENKA D, KOHÚT M (2001) Late Cretaceous age of the Rochovce Granite, Western Carpathians, constrained by U–Pb single-zircon dating in combination with cathodoluminescence imaging. *Geol Carpath* 52: 41–47
- PROTAS J (1957) Propriétés et synthèse d'un oxyde hydraté d'uranium et de calcium de Shinkolobwe, Katanga. *C R Acad Sci Paris* 244: 91–93
- PUTIŠ M, SERGEEV S, ONDREJKA M, LARIONOV A, SIMAN P, SPIŠIAK J, UHER P, PADERIN I (2008) Cambrian–Orдовician metaigneous rocks associated with Cadomian fragments in the West-Carpathian basement dated by SHRIMP on zircons: a record from the Gondwana active margin setting. *Geol Carpath* 59: 3–18

- RADVANEC M, GRECULA P (2016) Geotectonic and metallogenetic evolution of Gemicum (inner Western Carpathians) from Ordovician to Jurassic. *Miner Slov* 48: 105–118
- RADVANEC M, KONEČNÝ P, ONDREJKA M, PUTIŠ M, UHER P, NÉMETH Z (2009) The Gemic granites as an indicator of the crustal extension above the Late-Variscan subduction zone during the Early Alpine riftogenesis (Western Carpathians): an interpretation from the monazite and zircon ages dates by CHIME and SHRIMP methods. *Miner Slov* 41: 381–394
- ROJKOVIČ I (1997) Uranium Mineralization in Slovakia. Comenius University, Bratislava, pp 1–117
- ROJKOVIČ I, NOVOTNÝ L (1993) Uranium mineralization in Gemicum. *Miner Slov* 25: 368–370 (in Slovak)
- ROJKOVIČ I, PUŠKELOVÁ Ľ, KHUN M, MEDVEĎ J (1995) U–REE–Au in veins and black shales of the Gemicum, Slovakia. In: PAŠAVA J, KRÍBEK B, ŽÁK K (eds) *Mineral Deposits: From Their Origin to Their Environmental Impacts*. Balkema, Rotterdam, pp 789–792
- ROJKOVIČ I, HÁBER M, NOVOTNÝ L (1997) U–Au–Co–Bi–REE mineralization in the Gemic Unit (Western Carpathians, Slovakia). *Geol Carpath* 48: 303–313
- ROJKOVIČ I, KONEČNÝ P, NOVOTNÝ L, PUŠKELOVÁ Ľ, STREŠKO V (1999) Quartz–apatite–REE vein mineralization in Early Paleozoic rocks of the Gemic Superunit, Slovakia. *Geol Carpath* 50: 215–227
- SEJKORA J, PLÁŠIL J, BUREŠ B (2013) Unusual association of supergene uranium minerals from the Jan Evangelista vein, Jáchymov (Czech Republic). *Bull mineral-petrolog Odd Nár Muz (Praha)* 21: 143–156 (in Czech)
- SNOPKO L, IVANIČKA J (1978) Considerations on the paleogeography in the Lower Paleozoic of Spišsko-Gemerské Rudohorie Mts. In: VOZÁR J (ed) *Paleogeographical Evolution of the Western Carpathians*. Geological Institution of D. Štúr, Bratislava, pp 269–280 (in Slovak)
- ŠČERBINA VV (1963) Geochemistry of uranium in the oxidation zone. In: VINOGRADOV AP (ed.) *Basic Features of Uranium Geochemistry*. Publishing House of the AS USSR, Moscow, pp 220–237 (in Russian)
- ŠTEVKO M, UHER P, ONDREJKA M, OZDÍN D, BAČÍK P (2014) Quartz–apatite–REE phosphates–uraninite vein mineralization near Čučma (eastern Slovakia): a product of early Alpine hydrothermal activity in the Gemic Superunit, Western Carpathians. *J Geosci* 59: 209–222
- VAES JF (1947) Six nouveaux minéraux d'urane provenant de Shinkolobwe (Katanga). *Ann Soc géol Belg* 70: 212–225
- VARČEK C (1977) Some rare mineralization types in the Spišsko-Gemerské Rudohorie Mts. In: HÁBER M. (ed) *Ore-Forming Processes in the Western Carpathians*. Universitas Comeniana, Bratislava, pp 93–99 (in Slovak)
- VOZÁROVÁ A (1993) Variscan metamorphism and crustal evolution of the Gemicum. *Západ Karpaty, Sér Mineral Petrogr Geochém Metalogen* 16: 55–117 (in Slovak)
- VOZÁROVÁ A, ŠARINOVÁ K, SERGEEV S, LARIONOV A, PRESNYAKOV S (2010) Late Cambrian/Ordovician magmatic arc type volcanism in the Southern Gemicum basement, Western Carpathians, Slovakia: U–Pb (SHRIMP) data from zircons. *Int J Earth Sci* 99: 17–37
- VOZÁROVÁ A, RODIONOV N, ŠARINOVÁ K, PRESNYAKOV S (2017) New zircon ages on the Cambrian–Ordovician volcanism of the Southern Gemicum basement (Western Carpathians, Slovakia): SHRIMP dating, geochemistry and provenance. *Int J Earth Sci* 106: 2147–2170